3D Building Modelling from ALS Point Clouds by Delaunay Triangulation and Graph Theories

Gefei Kong[1], Hongchao Fan[1], Gabriele Lobaccaro[1]

[1] Department of Civil and Environmental Engineering, Norwegian University of Science and Technology, Trondheim, Norway - (gefei.kong, hongchao.fan, gabriele.lobaccaro)@ntnu.no

Keywords: 3D roof reconstruction, Rule-based, Graph analysis, Delaunay triangulation, Point clouds.

Abstract

As an important task in 3D building reconstruction, 3D roof reconstruction attracts increasing attention. Existing methods have the issue of additional errors caused by multi-step processes, resulting in relatively high uncertainty and potentially affecting the reconstruction accuracy. Deep learning-based methods to achieve the direct extraction of roof vertices and edges for reconstructing 3D roof structures tackle the issue of additional errors while leading to another problem: the reliance on large labeled datasets for training. In this study, a fully rule-based method is proposed to achieve automatic 3D roof reconstruction. Roof vertices with their edges parallel to the x-y plane are first extracted from the point clouds, and subsequently, the left roof edges connecting vertices are inferred by using Delaunay triangulation. Finally, the 3D roof structure is reconstructed by using graph analysis based on the information of roof vertices and edges. This method simplifies the process of 3D roof reconstruction, and the experiment results demonstrate that the proposed method can effectively reconstruct 3D roof structures from point clouds.

1. Introduction

In many fields such as urban planning and geographic simulation, 3D roof models play a crucial role as the foundation of 3D building models (Wang et al., 2018). As introduced in CityGML 2.0 (Gröger et al., 2012), the 3D roof information is considered in 3D building models from the level of detail 2 (LoD2) in five LoDs from 0 to 4. The task of 3D roof reconstruction from point clouds attracts much attention.

To address the task of 3D roof reconstruction from point clouds, numerous model-driven and data-driven methods are proposed. The flexibility of model-driven methods (Huang et al., 2013, Jarząbek-Rychard and Borkowski, 2016) is limited by their pre-defined roof primitives, resulting in the weak adaptation of changing architectural styles. In contrast, data-driven methods (Cao et al., 2017, Huang et al., 2022, Peters et al., 2022) are more flexible because they can achieve 3D roof reconstruction without pre-defined knowledge. However, additional errors are brought in and accumulated during the multi-step processes, increasing the uncertainty and ultimately affecting the accuracy of the reconstructed result. A solution to directly extract roof vertices and edges for 3D roof reconstruction decreases the number of steps and thus can reduce the accumulated errors. Some deep learning-based methods following this strategy (Li et al., 2022) have been proposed and achieved state-of-the-art performance in the task of 3D roof reconstruction. However, their reliance on large labeled training datasets affects their value in practical applications.

To tackle the issues of accumulated errors in traditional data-driven methods and the need for large labeled datasets in deep learning-based methods, a new rule-based method for 3D roof reconstruction based on roof vertex detection and edge prediction is proposed in this study. This method detects roof lines parallel to the x-y plane and roof vertices based on voxelization and neighborhood analysis, and further predicts the remaining roof lines and generates 3D roof structures by using Delaunay triangulation and graph analysis. The main highlights of this study are as follows.

1. The proposed method directly extracts roof vertices and infers roof edges from the point clouds. Without the additional roof plane segmentation and primitive extraction, the processes of 3D roof reconstruction are simplified and the potential errors accumulated during the multi-step processes in existing methods can be reduced.
2. The proposed method is rule-based and the extraction of roof vertices and edges is achieved without the need for training data, reducing the costs of preparation work and enhancing its applicability.

This paper is organized as follows. Section 2 reviews the related works of 3D roof reconstruction. In Section 3 the detailed workflow of the proposed method is described. Section 4 introduces the experiment settings, while Section 5 presents and discusses the experimental result. In Section 6, the conclusion of this study is presented and its further work is discussed.

2. Related Works

The methods for 3D roof reconstruction are generally divided into two types: model-driven and data-driven. Model-driven methods start from pre-defined roof primitives and then reconstruct 3D roofs by combining these pre-defined primitives and optimizing their parameters. (Huang et al., 2013) defined a library of roof primitives categorized into three groups consisting of eleven types. Subsequently, generative modelling was employed to reconstruct 3D roof models that fit the data. (Jarząbek-Rychard and Borkowski, 2016) proposed a library of building elementary structures with more flexible rules. This library was combined with the roof topology graph to identify topology and recognize pre-defined structures from the roof point clouds with segmented plane information, and finally achieved the 3D roof reconstruction. While model-driven methods exhibit robustness in reconstructing 3D roofs with complete topology, their flexibility is limited by the pre-defined parametric knowledge.

This contribution has been peer-reviewed. The double-blind peer-review was conducted on the basis of the full paper.
https://doi.org/10.5194/isprs-annals-X-4-2024-183-2024

Data-driven methods generally follow the workflow of roof plane segmentation, vector primitive tracing, and topology inference between roof planes, edges, and vertices. Many methods have been proposed and utilized to support this workflow. For example, region growing (Liu et al., 2023) and random sample consensus (RANSAC) (Canaz Sevgen and Karsli, 2020) for roof plane segmentation; convex-hull (Rhee and Williams, 2023) and α-shape (Chen et al., 2017) for obtaining vector primitives; and objective function and roof topology graph (Xiong et al., 2014) for final topology reconstruction. Without the requirement of pre-defined information, data-driven methods have better flexibility and generalization compared with model-driven methods. However, more steps and rules in data-driven methods cause new issues and affect the accuracy of reconstructed 3D roofs. The over- and under-segmentation issue in the roof plane segmentation step decreases the roof structure accuracy and would ultimately affect the practicality of the reconstruction result. This issue was also mentioned in the model-driven method (Jarząbek-Rychard and Borkowski, 2016) which included the roof plane segmentation step. Meanwhile, the process of obtaining vector primitives by boundary tracing or plane fitting relies on additional sub-steps and constraints, thereby bringing additional errors and uncertainty.

As mentioned in Section 1, the solution based on roof vertex and edge extraction can simplify the workflow of data-driven methods, thus mitigating the challenges associated with uncertainty and error accumulation. In the research by (Li et al., 2022), they proposed a two-stage deep neural network, Point2Roof, to extract roof vertices and predict edges from the roof point cloud. Their experiments on synthetic and real datasets demonstrate that Point2Roof successfully infers 3D roof structures and achieves state-of-the-art performance. However, the practicality and generalization of their deep learning-based method are limited by the requirement for large training datasets and fine-tuning.

3. Methodology

The proposed method aims to directly detect vertices and predict edges of building roofs from point clouds. The workflow consists of two major modules: (1) detection of roof vertices and their corresponding roof lines parallel to the x-y plane and (2) prediction of remaining roof edges and structure generation. Furthermore, the second module can be summarized as two sub-modules: (2.1) creation of Delaunay triangulation with segment constraints and obtaining basic cycles and (2.2) generation of 3D roof structures by obtaining roof faces through merging cycles based on graph analysis.

These modules are described in detail in Section 3.1 and 3.2. Meanwhile, this workflow is illustrated in Figure 1. The ”roof structure line” mentioned in Figure 1-”Module 1” denotes the roof lines parallel to x-y plane in this study and its example is shown by the red lines in Figure 1(b).

3.1 Extraction of Structure Lines and Roof Vertices

The extraction of roof structure lines and roof vertices is achieved by the method proposed in (Kong et al., 2023). This method utilizes the point clouds of a single roof as the input and does not require prior plane segmentation. First, the rotation based on the dominant direction and voxelization are implemented to regularize the point cloud data. Next, two rules for identifying voxels on or not on roof structure lines are designed and iteratively applied for each voxel, to achieve the detection of candidate voxels of potential roof structure lines. Subsequently, the roof structure lines of the input roof are determined based on these candidate voxels by five rules for candidate line extraction, clustering, and merging. Ultimately, the determined roof structure lines are segmented and their endpoints are extracted as the roof vertices.

The roof vertices and their corresponding structure line segments on the voxel coordinate system are saved and are utilized as the input of Module 2, and an example of these results is shown in Figure 1(b). Additionally, in the first step of this module, the rotation information is saved and transmitted to the next module, to re-rotate the generated structures to the geographic coordinate system.

3.2 Prediction of Roof Edges and Structure Generation

Roof vertices V and their corresponding structure line segments L from Section 3.1 provide a basic split of a roof’s point clouds. However, how to correctly connect these segments to create faces for structure generation remains an issue. Hence, this module should extract the left roof edges and further determine roof faces to ultimately generate the 3D roof structure. All these works in this module are divided into two sub-modules as mentioned above, and the detailed workflow is introduced as follows.

The first sub-module ”Create constrained Delaunay triangulation and find basic cycles” is used to connect all vertices by found edges and obtain the candidate face group of triangles. Delaunay triangulation is widely used in the field of surface reconstruction (Miao et al., 2019, Luo et al., 2021). In this study, it is employed to establish connections among roof vertices for reconstructing roof surfaces. However, roof vertices V are sparse and the Delaunay triangulation only based on them might lead to erroneous connection. To avoid this issue, the proposed method utilizes L to guide and constrain the triangulation process, as it is a subset of roof edges. An example of this constrained Delaunay triangulation is shown in Figure 1(c), where the red edges represent the segments L used for the constraints and the blue edges result from the triangulation process. In this way, the prediction of the remaining roof edges is achieved. Triangles formed by all these edges are regarded as the candidate roof faces. During this process, because L does not enclose the area to be triangulated, the triangulation will be implemented for the convex hull of V and L. This means that some unexpected triangles are also generated, where an example is shown in Figure 2. To tackle this issue, the proposed method calculates the α-shape of voxelized point clouds in 2D and utilizes it to assist in cleaning unexpected triangles. The cleaning strategy is: the triangles with intersection-area percentages between themselves and the α-shape polygon exceeding a specific threshold are saved, while those not meeting this criterion are removed. In this study, the threshold is set as 70%. The cleaned triangles are saved and regarded as the basic cycles T used in the next sub-module.

The second sub-module ”Merge cycles based on normals and graph analysis” is implemented to find roof faces and ultimately generate the 3D structure of a roof. Triangles (i.e., basic cycles T) obtained from the previous sub-module can compose a 3D roof but this outcome cannot precisely represent a roof structure due to over-segmentation. Therefore, in this sub-module,

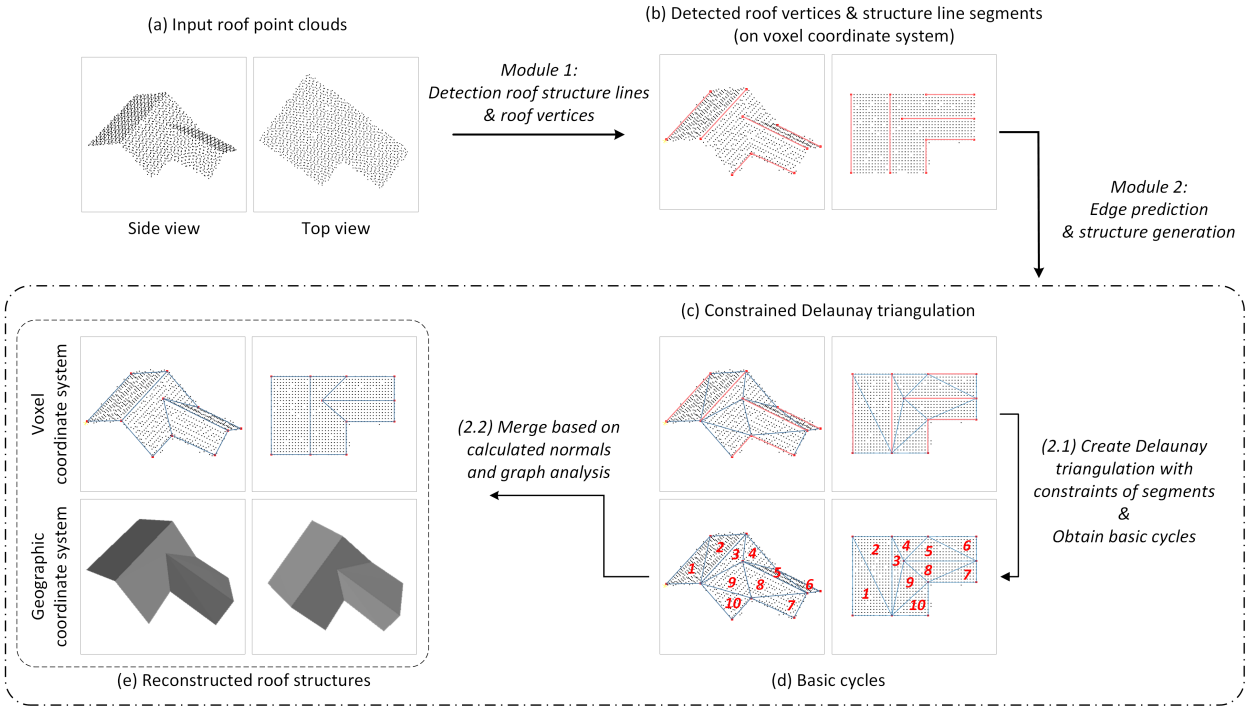

Figure 1. Workflow of the proposed method.

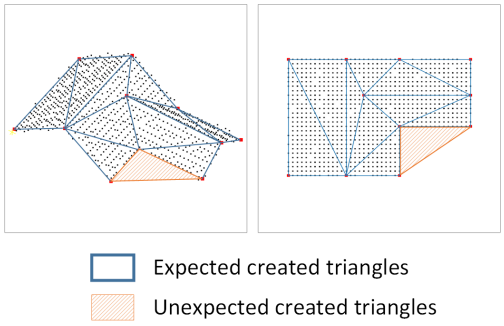

Figure 2. Example of unexpected triangles created in constrained Delaunay triangulation.

these basic cycles are further merged to obtain an accurate representation of roof faces. In this study, this merging process is achieved based on normals and can be summarized as the following four steps.

1. Calculate the normals of all triangles. The normals of planes vary with different orientations of the planes, thus can separate different roof faces. In this proposed method, the normals of triangles are calculated by singular value decomposition (SVD), which only relies on the vertex information of each triangle and does not require their order. These calculated normals are denoted as N.
2. Cluster normals to obtain the candidate face groups. The triangles that have similar normals are considered to belong to the same face. Following this principle, the candidate face groups are obtained by clustering these triangles based on their normals. The density-based spatial clustering (DBSCAN) algorithm is utilized to achieve this clustering of N, where ε is set to 0.3 and the minimum number of objects to form a cluster ($minPts$) is set to 1. The obtained candidate face groups are denoted as $G = \{g = \{t\} | \{t\} \subseteq T\}$. For an example shown in Figure 1(d), there is a $g = \{t_1, t_2\}$ for triangles 1 and 2.
3. Merge each candidate face group to generate the roof face. The merging of triangles in a candidate face group g is accomplished based on graph theory. g includes multiple triangles, consisting of a series of vertices and edges. Consequently, it can be conceptualized as an undirected graph and denoted as $g = \{t\} = \{\langle V_g, E_g \rangle\}$. In graph theory, a ”cycle” is defined as a non-empty path that starts and ends at the same node, with no repeated nodes in between (Bacciu et al., 2020). The cycle concept is similar to ”polygon” in the geographic field and thus can be extended to that. Hence, the challenge of merging a face group can be transformed into the identification of the largest cycle in a face graph, where the ”largest” means the cycle with the largest area. In this step, all potential cycles in g are first founded using a classic algorithm depth-first search (DFS). Subsequently, the cycle with the maximum area is extracted as the generated face f of g and f is appended to a set $\{f\}_g$ for the next sub-step. Following this, the process is iterated considering the scenario where g has the potential to cover multiple faces with the same normal (i.e., $g - \{f\}_g \neq \varnothing$). The iteration stops when $g - \{f\}_g$ is empty, indicating that all vertices and edges in g have been considered. The obtained face set $\{f\}_g$ represents the generated roof faces from the corresponding candidate face group g. For an example shown in Figure 1(d), the $\{f\}_{g=\{t_1,t_2\}}$ corresponds to one output face.
4. By repeating the third step and merging all candidate face groups, all roof faces $\{\{f\}_g\}$ are obtained and will be used for the final generation of 3D roof structures.

Ultimately, the 3D structure of this roof can be generated by using the face information $\{\{f\}_g\}$ and the vertices V_f included in $\{\{f\}_g\}$. However, the vertices in this result are still in the voxel coordinate system, as shown in the first row of Figure 1(e). To output the geographic 3D roof structure, these vertices V_f in

https://doi.org/10.5194/isprs-annals-X-4-2024-183-2024

the voxel coordinate system are re-rotated to the geographic coordinate system based on the rotation information calculated in Section 3.1. An example of the generated geographic 3D roof structure is shown in the second row of Figure 1(e).

4. Experiment Settings

To qualitatively and quantitatively evaluate the performance of the proposed method, the experiment is conducted on the dataset outlined in Section 4.1. The metrics for quantitative evaluation are introduced in Section 4.2.

4.1 Experimental Dataset

A dataset including 50 roofs is created for the experiments. Raw airborne laser scanning (ALS) point cloud data used in this dataset is located in Trondheim, Norway, and was collected in 2018. Based on the data collection place, the dataset is named as ”Trondheim” dataset in this study. The point density of the raw point clouds is 12–20 points/m^2. This data is provided by the mapping authority of Trondheim Municipality. The manually annotated 3D roof structures of these 50 roofs are employed as the ground truth data. Multiple roof structure types from primary (e.g. gabled and hipped) to complex (e.g. T-shaped, L-shaped, and combined) are covered in the experimental dataset, to ensure the comprehensive evaluation.

4.2 Evaluation Metrics

The following evaluation metrics are selected for the quantitative evaluation: vertex distance errors in x-, y- and z- dimensions (vd_x, vd_y, vd_z) for geometry accuracy evaluation and precision (P) and recall (R) for overall accuracy evaluation. The precision and recalls of detected vertices and predicted edges are considered separately, and present as VP and VR for vertex evaluation and EP and ER for edge evaluation.

The detailed calculation methods of these metrics follow (Li et al., 2022) and (Kong et al., 2023). A true positive vertex in these metrics is the detected vertex whose minimum distance to ground truth vertices is smaller than a pre-defined threshold. In this study, this threshold is set as 1 m. The true positive edges are similarly defined with the same threshold.

5. Experimental Results

5.1 Qualitative Evaluation Results

The qualitative evaluation results on the Trondheim dataset are shown in Figure 3. The colored points in Figure 3(a) and black points in Figure 3(b) represent the roof point clouds. The black points and edges in Figure 3(a) form the ground-truth 3D structures of these roofs. The red points in Figure 3(b) represent the detected vertices by Section 3.1. The generated 3D roof structures by the proposed method in this study is shown in Figure 3(c).

Overall, the qualitative results shown in Figure 3 demonstrate that the proposed method can effectively reconstruct 3D roof structures from point clouds. The complete and accurate 3D roof structures are successfully reconstructed by the proposed method in the face of both primary roof types such as gabled (R1) and hipped (R2) and complex roof types such as L-shaped (R3) and T-shaped (R4), although the proposed method performs not as perfect as the other cases in the face of a combined case shown by R5. For R5, its main problems are missing a triangle as shown by the purple box in Figure 3(c), and an additional generated roof face as shown by the orange box in Figure 3(c). The former is caused by an un-detected vertex in the module of roof vertex detection that is also illustrated by the purple box in Figure 3(b), while the latter is because this unexpected triangle is in the α-shape of this roof's point clouds. In addition, some unexpected vertices are detected in R4 as shown by the blue boxes in Figure 3(b). These vertices do not affect the representation of the reconstructed roof structure and do not bring additional sub-surface. However, they reduce the accuracy of the final reconstruction result.

5.2 Quantitative Evaluation Results

Type	Geometry (m)			Overall (%)	
	vd_x	vd_y	vd_z	P	R
vertex (V)	0.22	0.25	0.15	64.81	85.66
edge (E)	-	-	-	45.16	66.41

Table 1. Quantitative evaluation results on the Trondheim dataset

The quantitative evaluation results on the Trondheim dataset are shown in Table 1. As shown in the first row of Table 1, for roof vertex detection, the proposed method achieves 0.22 m of vd_x, 0.25 m of vd_y, and 0.15 m of vd_z for geometry accuracy; and 64.81% of VP and 85.66% of VR for overall accuracy evaluation. These results indicate that the proposed method can effectively and accurately extract roof vertices. For roof edge prediction whose results are shown in the second row of Table 1, the proposed method achieves 45.16% of EP and 66.41% of ER.

While the proposed method performs well on the reconstruction of 3D roof structures, compared to the overall evaluation results of vertex detection, those of edge prediction are lower by 19.65% on precision and 19.25% on recall. This implies that the proposed method exhibits worse performance in edge prediction. This gap is primarily caused by error accumulation and amplification from vertex detection to edge prediction, as a wrongly detected vertex has the potential to affect at least two edges. This issue is illustrated by the purple boxes of R5 in Figure 3, where a roof vertex that is not detected finally leads to a missing triangle in the reconstruction result and further results in the incorrect prediction of its two related edges. Additionally, the relatively low precision of vertex detection implies that additional vertices that are not correct or along the roof edge might be detected. The roof lines corresponding to these vertices lead to additional and incorrect constraints of Delaunay triangulation, while the triangulation process is the foundation of other edges' prediction. The inference of the 3D roof structure thus is impacted ultimately. The potential solution to this issue is improving the edge prediction process by optimization algorithms. By designing an objective function to minimize the distance between the raw point clouds and the reconstructed 3D roof structures, the wrongly detected vertices with their corresponding roof lines can be removed and the missing vertices can be identified and added, and finally achieve the more accurate edge prediction.

Nevertheless, when further analysing the value distribution of EP and ER by their histograms as shown in Figure 4 and 5, we can find that the proposed method achieves quite good results of EP and ER on most roofs. The percentages of reconstructed roof structures whose EP and ER are over 50% achieve 52%

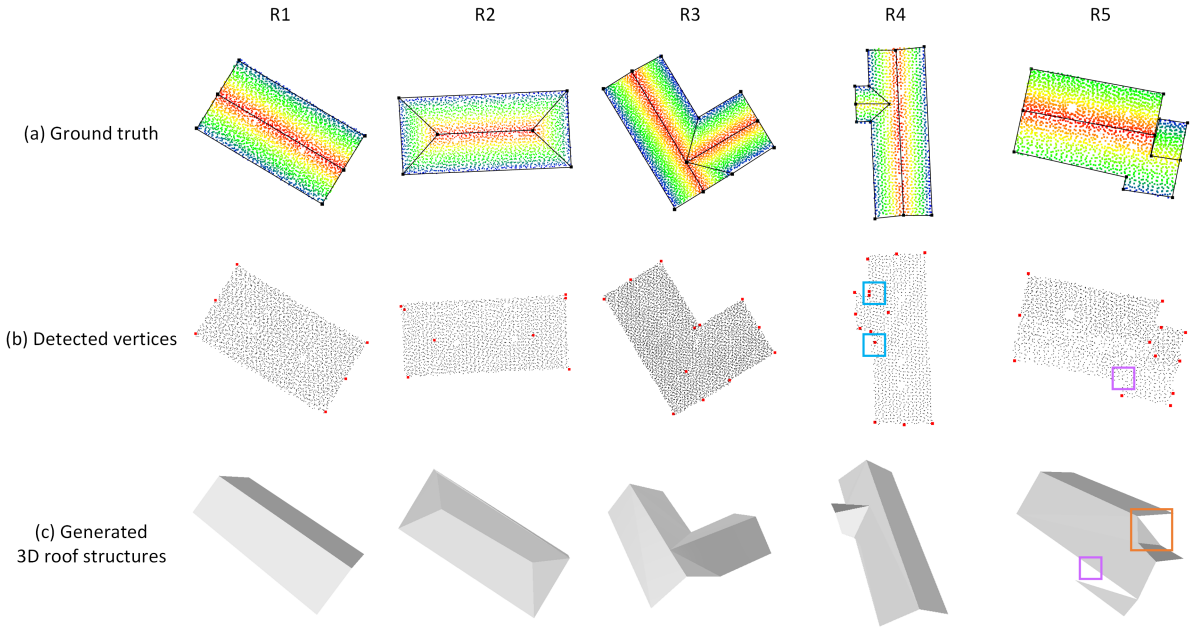

Figure 3. Qualitative evaluation results on the Trondheim dataset.

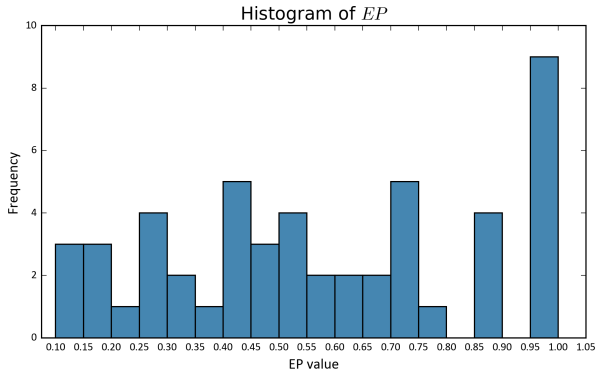

Figure 4. Histogram of EP.

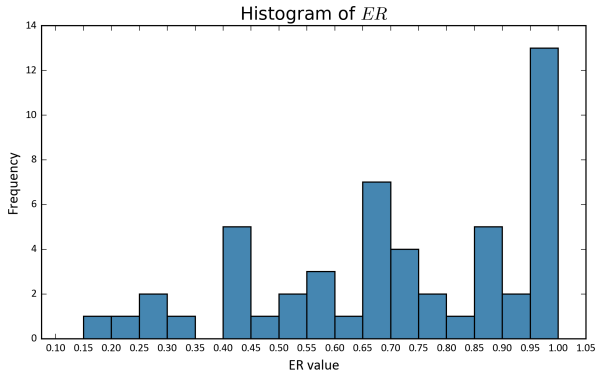

Figure 5. Histogram of ER.

and 76%, respectively. This analysis result indicates that, although the proposed method appears to perform less optimally in edge prediction compared to vertex detection on the overall evaluation, it is still capable of achieving acceptable edge prediction performance in most cases.

6. Conclusion

In this study, a new rule-based method for 3D roof structure reconstruction based on point cloud data is proposed. In the proposed method, instead of following the traditional workflow for this task, including roof plane segmentation, primitive extraction, and topology analysis, a more straightforward strategy is applied. This new strategy only includes two modules for roof vertex detection and edge prediction (structure generation). Vertex rules are first defined and implemented to detect roof vertices and extract their corresponding roof structure lines. With the constraints of these structure lines, constrained Delaunay triangulation is created and the candidate face groups are found based on the rules of normals. The final 3D roof structures are ultimately generated after merging the faces in each group through graph analysis. Having fewer number of modules reduces the potential for accumulated errors. The characteristic of the proposed method, which does not require a training process or data, further ensures its practicability and generalization. The qualitative and quantitative experimental results on the Trondheim dataset demonstrate the effectiveness of the proposed method. However, this method still faces some challenges. The errors from mis-detected or un-detected vertices are still accumulated to the next step of edge prediction and finally reduce the accuracy of reconstructed 3D roof structures. Additionally, the triangles for structure generation are still not clean enough, which leads to some additional faces being reconstructed. The potential solution to these issues is adding a sub-module to review the consistency of created constrained Delaunay triangulation of a roof and its corresponding point clouds. Furthermore, the issue of mis-detected vertices can also be managed through polygon simplification.

In the future, besides further improving the proposed method based on the abovementioned analysis, this 3D reconstruction method of roof structures will be employed for the automatically large-scale 3D building modelling in LoD2. Further applications of the 3D roof and building models, such as solar energy analysis, will also be explored, to implement this method in the real world.

This contribution has been peer-reviewed. The double-blind peer-review was conducted on the basis of the full paper.
https://doi.org/10.5194/isprs-annals-X-4-2024-183-2024 | © Author(s) 2024. CC BY 4.0 License.

Acknowledgements

The authors would like to thank the mapping authority of Trondheim Municipality who provided the point cloud data in Trondheim, Norway. The work in this paper is supported by NTNU Digital project (project No. 81771593) and the Research Council of Norway project FRIPRO FRINATEK HELIOS - enHancing optimal ExpLoitatIOn of Solar energy in Nordic cities through digitalization of built environment (project No. 324243).

References

Bacciu, D., Errica, F., Micheli, A., Podda, M., 2020. A gentle introduction to deep learning for graphs. *Neural Networks*, 129, 203–221.

Canaz Sevgen, S., Karsli, F., 2020. An improved RANSAC algorithm for extracting roof planes from airborne lidar data. *The Photogrammetric Record*, 35(169), 40–57.

Cao, R., Zhang, Y., Liu, X., Zhao, Z., 2017. 3D building roof reconstruction from airborne LiDAR point clouds: a framework based on a spatial database. *International Journal of Geographical Information Science*, 31(7), 1359–1380.

Chen, D., Wang, R., Peethambaran, J., 2017. Topologically Aware Building Rooftop Reconstruction From Airborne Laser Scanning Point Clouds. *IEEE Transactions on Geoscience and Remote Sensing*, 55(12), 7032–7052.

Gröger, G., Kolbe, T. H., Nagel, C., Häfele, K.-H., 2012. Ogc city geography markup language (citygml) encoding standard. Version 2.0, OGC Doc No. 12–019, Open Geospatial Consortium.

Huang, H., Brenner, C., Sester, M., 2013. A generative statistical approach to automatic 3D building roof reconstruction from laser scanning data. *ISPRS Journal of Photogrammetry and Remote Sensing*, 79, 29–43.

Huang, J., Stoter, J., Peters, R., Nan, L., 2022. City3D: Large-Scale Building Reconstruction from Airborne LiDAR Point Clouds. *Remote Sensing*, 14(99), 2254.

Jarząbek-Rychard, M., Borkowski, A., 2016. 3D building reconstruction from ALS data using unambiguous decomposition into elementary structures. *ISPRS Journal of Photogrammetry and Remote Sensing*, 118, 1–12.

Kong, G., Zhao, Y., Fan, H., 2023. Detecting vertices of building roofs from ALS point cloud data. *International Journal of Digital Earth*, 16(2), 4811–4830.

Li, L., Song, N., Sun, F., Liu, X., Wang, R., Yao, J., Cao, S., 2022. Point2Roof: End-to-end 3D building roof modeling from airborne LiDAR point clouds. *ISPRS Journal of Photogrammetry and Remote Sensing*, 193, 17–28.

Liu, K., Ma, H., Zhang, L., Liang, X., Chen, D., Liu, Y., 2023. Roof Segmentation From Airborne LiDAR Using Octree-Based Hybrid Region Growing and Boundary Neighborhood Verification Voting. *IEEE Journal of Selected Topics in Applied Earth Observations and Remote Sensing*, 16, 2134–2146.

Luo, Y., Mi, Z., Tao, W., 2021. DeepDT: Learning Geometry From Delaunay Triangulation for Surface Reconstruction. *Proceedings of the AAAI Conference on Artificial Intelligence*, 35(3), 2277–2285.

Miao, W., Liu, Y., Shi, X., Feng, J., Xue, K., 2019. A 3d surface reconstruction method based on delaunay triangulation. Y. Zhao, N. Barnes, B. Chen, R. Westermann, X. Kong, C. Lin (eds), *Image and Graphics*, Lecture Notes in Computer Science, Springer International Publishing, Cham, 40–51.

Peters, R., Dukai, B., Vitalis, S., van Liempt, J., Stoter, J., 2022. Automated 3D Reconstruction of LoD2 and LoD1 Models for All 10 Million Buildings of the Netherlands. *Photogrammetric Engineering & Remote Sensing*, 88(3), 165–170.

Rhee, J., Williams, B., 2023. Cost-effective 3d urban massing reconstruction of public aerial lidar scans. M. Turrin, C. Andriotis, A. Rafiee (eds), *Computer-Aided Architectural Design. INTERCONNECTIONS: Co-computing Beyond Boundaries*, Communications in Computer and Information Science, Springer Nature Switzerland, Cham, 207–218.

Wang, R., Peethambaran, J., Chen, D., 2018. LiDAR Point Clouds to 3-D Urban Models: A Review. *IEEE Journal of Selected Topics in Applied Earth Observations and Remote Sensing*, 11(2), 606–627.

Xiong, B., Oude Elberink, S., Vosselman, G., 2014. A graph edit dictionary for correcting errors in roof topology graphs reconstructed from point clouds. *ISPRS Journal of Photogrammetry and Remote Sensing*, 93, 227–242.